Neurobiology of Disease

$P2X_7$ Receptor Blockade Prevents ATP Excitotoxicity in Oligodendrocytes and Ameliorates Experimental Autoimmune Encephalomyelitis

Carlos Matute,[1] Iratxe Torre,[1] Fernando Pérez-Cerdá,[1] Alberto Pérez-Samartín,[1] Elena Alberdi,[1] Estibaliz Etxebarria,[1] Amaia M. Arranz,[1] Rivka Ravid,[2] Alfredo Rodríguez-Antigüedad,[3] MaríaVictoria Sánchez-Gómez,[1] and María Domercq[1]

[1]Departamento de Neurociencias, Universidad del País Vasco, 48940 Leioa, Spain, [2]Netherland Brain Bank, 1105 AZ Amsterdam ZO, The Netherlands, and [3]Servicio de Neurología, Hospital de Basurto, 48008 Bilbao, Spain

Oligodendrocyte death and demyelination are hallmarks of multiple sclerosis (MS). Here we show that ATP signaling can trigger oligodendrocyte excitotoxicity via activation of calcium-permeable $P2X_7$ purinergic receptors expressed by these cells. Sustained activation of $P2X_7$ receptors *in vivo* causes lesions that are reminiscent of the major features of MS plaques, i.e., demyelination, oligodendrocyte death, and axonal damage. In addition, treatment with $P2X_7$ antagonists of chronic experimental autoimmune encephalomyelitis (EAE), a model of MS, reduces demyelination and ameliorates the associated neurological symptoms. Together, these results indicate that ATP can kill oligodendrocytes via $P2X_7$ activation and that this cell death process contributes to EAE. Importantly, $P2X_7$ expression is elevated in normal-appearing axon tracts in MS patients, suggesting that signaling through this receptor in oligodendrocytes may be enhanced in this disease. Thus, $P2X_7$ receptor antagonists may be beneficial for the treatment of MS.

Key words: **oligodendrocytes; ATP; excitotoxicity; demyelination; EAE; multiple sclerosis**

Introduction

Multiple sclerosis (MS) is a chronic, degenerative disease of the CNS that is characterized by focal lesions with inflammation, infiltration of immune cells, demyelination, oligodendroglial death, and axonal damage (Prineas et al., 2002). These cellular alterations are accompanied by neurological deficits such as sensory disturbances, lack of motor coordination, and visual impairment. MS is thought to usually begin with an autoimmune inflammatory reaction to myelin components and progresses later to a chronic phase in which oligodendrocytes, myelin, and axons degenerate (Steinman, 2001; Lassmann, 2005). Both genetic and environmental factors contribute to MS susceptibility (Zamvil and Steinman, 2003). Among them, primary and/or secondary alterations in glutamate signaling cause excitotoxicity that contributes to MS pathology (Matute et al., 2001; Groom et al., 2003).

Like glutamate, extracellular ATP is a major excitatory neurotransmitter in the CNS, activating ionotropic (P2X) and metabotropic (P2Y) receptors (Burnstock, 1972; Ralevic and Burnstock, 1998; North, 2002). ATP-gated P2X channels are formed by $P2X_1$–$P2X_7$ subunits and have marked Ca^{2+} permeability (Torres et al., 1999; North, 2002). P2X receptors are expressed in CNS neurons, where they participate in fast synaptic transmission and modulation (Khakh, 2001). In addition, $P2X_7$ receptors mediate immunomodulatory responses (Di Virgilio et al., 1999) and signaling cascades, leading to neurodegeneration after ischemia (Le Feuvre et al., 2003). Recently, it has also been shown that spinal cord injury is associated with prolonged $P2X_7$ receptor activation, which results in neuronal excitotoxicity (Wang et al., 2004).

Because oligodendrocytes are vulnerable to glutamate excitotoxicity, we examined whether ATP, which also activates ionotropic receptors with calcium permeability, is toxic to these cells and whether it can cause demyelination. Here, we report that (1) oligodendrocytes and myelin express functional $P2X_7$ receptors that can mediate cell death *in vitro* and *in vivo*, (2) activation of $P2X_7$ receptors contributes to tissue damage in experimental autoimmune encephalomyelitis (EAE) pathology, and (3) $P2X_7$ receptor expression is increased in MS before lesion formation.

Materials and Methods

Oligodendrocyte cultures. Primary cultures of oligodendrocytes derived from optic nerves of 12-d-old Sprague Dawley rats were obtained as described previously (Barres et al., 1992). Cells were seeded into 24-well plates bearing 12-mm-diameter coverslips coated with poly-D-lysine (10 μg/ml) at a density of 5×10^3 cells per well. Cells were maintained at 37°C and 5% CO_2 in a chemically defined medium (Barres et al., 1992). After 2–4 d *in vitro*, cultures were composed of at least 98% O4/galactocerebroside-positive (O4/GalC$^+$) cells; the majority of the re-

Received Feb. 9, 2007; revised July 12, 2007; accepted July 13, 2007.

This work was supported by grants from the Ministerio de Sanidad, Ministerio de Educación y Ciencia, Gobierno Vasco, and Universidad del País Vasco. I.T., M.D., and E.E. held a fellowship from the Gobierno Vasco, and A.M.A. held a fellowship from the Ministerio de Sanidad y Consumo. E.A. is a Ramón y Cajal research fellow. We thank Dr. A. Verkhratsky and D. J. Fogarty for critical reading of this manuscript.

Correspondence should be addressed to Carlos Matute, Departamento de Neurociencias, Universidad del País Vasco, 48940 Leioa, Spain. E-mail: carlos.matute@ehu.es.

DOI:10.1523/JNEUROSCI.0579-07.2007

 0270-6474/07/279525-09$15.00/0

maining cells were stained with antibodies to glial fibrillary acidic protein (GFAP). No A2B5$^+$ or microglial cells were detected in these cultures (Alberdi et al., 2002).

Electrophysiology. Whole-cell recordings were performed at room temperature using the EPC-7 patch-clamp amplifier (HEKA Elektronik, Lambrecht, Germany). Currents were recorded at a holding membrane potential of −70 mV. Extracellular bath solution with a pH of 7.3 contained the following (in mM): 140 NaCl, 5.4 KCl, 2 $CaCl_2$, 1 $MgCl_2$, and 10 HEPES. Divalent cation-free extracellular solutions were obtained by omitting Ca^{2+} and Mg^{2+}. Patch-clamp pipettes (3–5 MΩ) were filled with internal solution at a pH of 7.3 containing the following (in mM): 140 CsCl, 2 $CaCl_2$, 2 $MgCl_2$, 10 HEPES, 11 EGTA, and 2 Na-ATP.

Measurement of $[Ca^{2+}]_i$. $[Ca^{2+}]_i$ was determined according to the method described previously (Grynkiewikcz et al., 1985). Oligodendrocytes were loaded with fura-2 AM (5 μM; Invitrogen, Carlsbad, CA) in culture medium for 30 min at 37°C. Cells were washed in HBSS containing 20 mM HEPES, pH 7.4, 10 mM glucose, and 2 mM $CaCl_2$ (incubation buffer) for 5 min at room temperature. Experiments were performed in a coverslip chamber continuously perfused with incubation buffer at 1 ml/min. The perfusion chamber was mounted on the stage of a Zeiss (Oberkochen, Germany) inverted epifluorescence microscope (Axiovert 35), equipped with a 150 W xenon lamp Polychrome IV (T.I.L.L. Photonics, Martinsried, Germany) and a Plan Neofluar 40× oil immersion objective (Zeiss). Cells were visualized with a high-resolution digital black/white CCD camera (ORCA; Hamamatsu Photonics Iberica, Barcelona, Spain), and image acquisition and data analysis were performed using the AquaCosmos software program (Hamamatsu Photonics Iberica). $[Ca^{2+}]_i$ was estimated by the 340/380 ratio method, using a K_d value of 224 nM. At the end of the assay, *in situ* calibration was performed with the successive addition of 10 mM ionomycin and 2 M Tris/50 mM EGTA, pH 8.5. Data were analyzed with Excel (Microsoft, Seattle, WA) and Prism (GraphPad Software, San Diego, CA) software.

Cell viability and toxicity assays. Cell toxicity and viability assays were performed as described previously (Sánchez-Gómez and Matute, 1999). Cells at 2–4 d in culture were exposed for 15 min to P2X receptor agonists. Antagonists were added to the cultures 15 min before the agonists. Twenty-four hours after drug application, cell viability was assessed using calcein-AM (Invitrogen). The total number of surviving cells on each coverslip emitting calcein fluorescence was counted, and results were expressed as percentage of cell death versus control. Results were expressed as the mean ± SEM of at least three independent experiments performed in duplicate.

Immunochemistry. Oligodendroglial expression of $P2X_7$ receptor was examined by double immunofluorescence applied to cultured oligodendrocytes and tissue from the rat optic nerve and spinal cord. Oligodendrocyte cultures were fixed in 4% paraformaldehyde in PBS and processed for immunocytochemistry as described previously (Matute et al., 1997). For tissue, adult Sprague Dawley rats were deeply anesthetized with chloral hydrate (500 mg/kg, i.p.) and transcardially perfused with 0.1 M sodium phosphate buffer (PB), pH 7.4, followed by 4% paraformaldehyde in the same buffer. Optic nerve and spinal cord samples and blocks containing hippocampus and adjacent cortex, the latter structures being used as positive controls, were dissected out and postfixed for 1 h in the same solution.

Primary antibodies were as follows: $P2X_1$, $P2X_2$, $P2X_4$, and $P2X_7$ (1–2 μg/ml; Alomone Labs, Jerusalem, Israel), $P2X_3$ (1 μg/ml; Chemicon, Temecula, CA), $P2X_5$ and $P2X_6$ (1:1000; Santa Cruz Biotechnology, Santa Cruz, CA), myelin basic protein (MBP) (1 μg/ml; Sternberger Monoclonals, Berkeley, CA), and adenomatous polyposis coli antigen (APC) (1 μg/ml; Calbiochem, Barcelona, Spain), an oligodendrocyte marker (Bhat et al., 1996).

Controls in oligodendrocyte cultures as well as in tissue sections were performed by either omitting the primary antibody or preadsorbing the primary antibody with an excess of the corresponding peptide (50 μg/ml final concentration). Labeling in hippocampus and cerebral cortex was similar to that obtained by other studies (Rubio and Soto, 2001). For double-immunofluorescence assays, after incubation with the suitable primary antibody as described above, sections were incubated with fluorescent goat anti-rabbit secondary antibody (Alexa Fluor 488; 1:200; Invitrogen). Subsequently, sections were incubated for 2 h at 37°C with mouse monoclonal antibody APC (1 μg/ml; Calbiochem), and labeling was revealed with fluorescent goat anti-mouse secondary antibody (Alexa Fluor 546; 1:200; Invitrogen).

For Western blots, samples (10 μg of protein per lane) of rat optic nerve cultures and tissue and human optic nerves were loaded and size separated in 10% SDS-PAGE. Proteins were blotted onto nitrocellulose filters (GE Healthcare, Little Chalfont, UK) and incubated with antibodies directed against $P2X_7$ (0.3 μg/ml, intracellular epitope), MBP (0.8 μg/ml; Sternberger Monoclonals, Berkeley, CA), and β-actin (1:1000; Sigma, Madrid, Spain). Immunoblots were visualized using enhanced chemiluminescence (Pierce, Rockford, IL). Protein band densitometry was performed using Scion Image for Windows (Scion, Frederick, MD), and actin immunoreactivity was used to normalize $P2X_7$ and MBP signal.

Immunogold electron microscopy. Three adult Sprague Dawley rats (250–300 g) were deeply anesthetized by intraperitoneal injection of 20% chloral hydrate in distilled water and transcardially perfused with 4% paraformaldehyde and 0.25% glutaraldehyde in 0.1 M PB, pH 7.4. Both longitudinal and transversal vibratome sections (60–70 μm thick) were osmicated in 1% osmium tetroxide in 0.1 M PB, dehydrated, and embedded in epoxy resins. Ultrathin sections were cut with a Reichert ultramicrotome and mounted on nickel grids. Ultrathin sections were processed for immunocytochemistry as described previously in detail (Somogyi and Soltész, 1986).

Incubation with primary antibodies to the intracellular and to the extracellular portion of $P2X_7$ receptors (1 μg/ml; Alomone Labs) were done overnight at 4°C followed with Auroprobe EM goat anti-rabbit IgG (heavy and light chains) 15 nm gold (1:20; GE Healthcare) for 1–2 h at room temperature. Sections were counterstained with 1% uranyl acetate and 1% lead citrate and examined using a Philips (Aachen, Germany) EM208S electron microscope.

Quantification was performed by taking microphotographs ($n = 122$) from three independent experiments. Scion Image software (National Institutes of Health, Frederick, MD) was used to measure the area of each cellular element and the number of gold particles inside them, and thus to calculate particle density (particles per square micrometer). Immunolabeling was absent when omitting the primary antibody.

Drug treatment of isolated and in vivo *optic nerves.* Isolated adult optic nerves from Sprague Dawley rats were perfused with oxygen-saturated artificial CSF (aCSF) (in mM: 126 NaCl, 3 KCl, 2 $MgSO_4$, 26 $NaHCO_3$, 1.25 NaH_2PO_4, and 2 $CaCl_2$ $2H_2O$) containing agonists and antagonists and subsequently processed for chromatin staining with Hoechst 33258 (5 μg/ml) and immunohistochemistry as described previously (Sánchez-Gómez et al., 2003). The results are the mean ± SEM of at least three different experiments performed in duplicate. The total number of fields counted for each treatment was 120.

For application of drugs or vehicle (saline) to the optic nerve *in vivo*, rabbits were anesthetized and infused with ATP-γ-S or 2′,3′-*O*-(benzoyl-4-benzoyl)-ATP (BzATP) (10 mM) alone or in conjunction with brilliant blue G (BBG) (10 μM) or oxidized ATP (oATP) (1 mM) as described previously in detail (Matute, 1998). Agonists (Sigma) were diluted in sterile PBS (145 mM NaCl in 10 mM phosphate buffer, pH 7.2) and slowly delivered through a cannula implanted under the optic nerve dura mater and attached to a plastic tube connected to a subcutaneously implanted osmotic pump (rate 1 μl/h over 2–3 d; Alzet; Alza, Cupertino, CA). Under these delivery conditions, the estimated concentration bathing the area surrounding the cannula is between two to three orders of magnitude lower than that loaded in the osmotic pump (Matute, 1998). After 7 d, animals were fixed with 4% paraformaldehyde, and optic nerves were analyzed by immunohistochemistry with antibodies to glial cells, myelin, and neurofilaments. The following mouse monoclonal antibodies were used: anti-MBP (0.8 μg/ml; Sternberger Monoclonals, Lutherville, MD), anti-neurofilament heavy chain (NFH) (1:10,000; Sternberger Monoclonals, Lutherville, MD), anti-GFAP (10 μg/ml; DakoCytomation, Glostrup, Denmark), anti-3′-5′cyclic nucleotide phosphodiesterase (CNPase) (7 μg/ml; Sigma), and finally APC (1 μg/ml; Calbiochem), a marker for oligodendrocyte cell bodies. CNPase and APC immunostaining was performed after a 20 min Pronase treatment at 37°C (protease type XIV, 50 μg/ml; Sigma). Binding of the antibodies

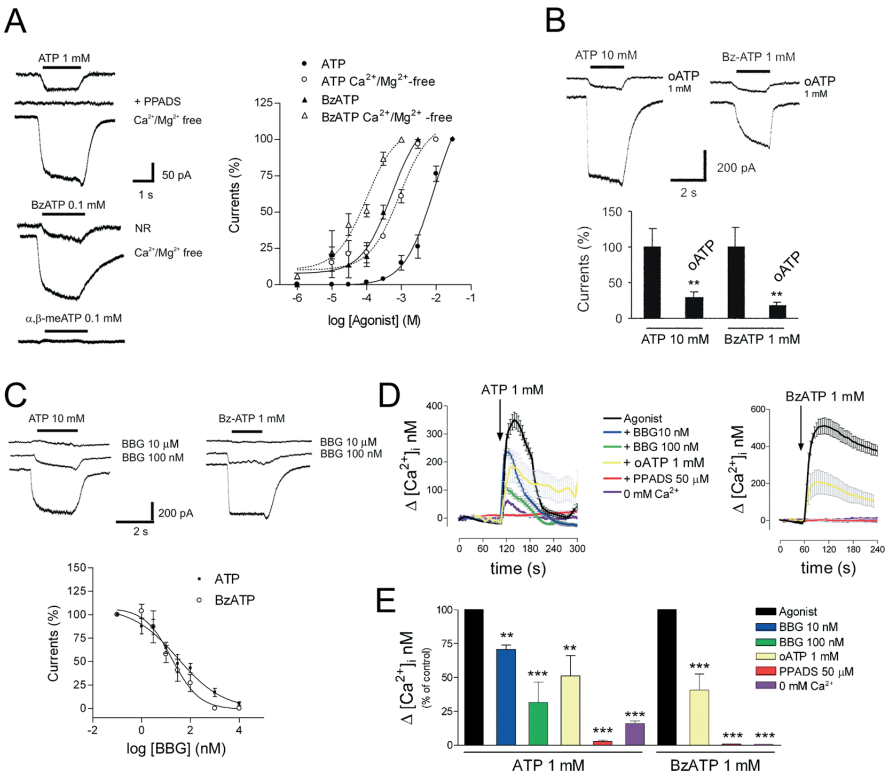

Figure 1. Oligodendrocytes express functional P2X receptors with high Ca^{2+} permeability. ***A***, ATP and BzATP, but not α,β-meATP, evoke inward, nondesensitizing currents, which are potentiated in the absence of Ca^{2+} and Mg^{2+}. ATP currents are blocked by PPADS (100 μM), a nonselective P2X antagonist. ***B***, ***C***, The $P2X_7$ antagonists oATP (1 mM) and BBG block ATP and BzATP currents. $^{**}p < 0.01$. ***D***, ***E***, ATP and BzATP induce a rapid increase in $[Ca^{2+}]_i$, an effect that is blocked by PPADS (50 μM) and in Ca^{2+}-free incubation buffer, and greatly reduced by the $P2X_7$ antagonists oATP (1 mM) and BBG (100 nM). $^{**}p < 0.01$ and $^{***}p < 0.001$.

was revealed using the avidin–biotin–peroxidase complex (Vector Laboratories, Burlingame, CA). Isolectin B4 histochemistry (1:20; Sigma) was used to identify cells of microglia/macrophage lineage. In each case, a parallel series of sections was processed for toluidine blue staining.

EAE induction and treatment. Chronic, relapsing EAE was induced in C57BL/6 mice by immunization with 300 μl of myelin oligodendrocyte glycoprotein 35–55 [MOG(35–55)] (200 μg; Sigma) in incomplete Freund's adjuvant supplemented with 8 mg/ml *Mycobacterium tuberculosis* H37Ra. Pertussis toxin (500 ng; Sigma) was injected on the day of immunization and again 2 d later. Mice were treated with oATP every 12 h (5 mg/kg, i.p., per day) or with BBG (10 mg/kg per day, delivered from pellets; IRA, Sarasota, FL) from 21 to 40 d post-immunization (dpi).

In all instances, motor symptoms were recorded daily and scored as follows from 0 to 8: 0, no detectable changes in muscle tone and motor behavior; 1, flaccid tail; 2, paralyzed tail; 3, impairment or loss of muscle tone in hindlimbs; 4, hindlimb hemiparalysis; 5, complete hindlimb paralysis; 6, complete hindlimb paralysis and loss of muscle tone in forelimbs; 7, tetraplegia; and 8, moribund. Conduction velocity of the corticospinal tract was assessed in anesthetized mice with tribromoethanol (240 mg/kg, i.p.; Sigma) using stimulatory and recording electrodes placed in the primary motor cortex and in the vertebral canal at the L2 level, respectively. After recording, mice were fixed, and spinal cord was processed for immunohistochemistry. Tissue blocks of spinal cords were cryoprotected, cut longitudinally (10 μm thick), and stained with toluidine blue and antibodies to MBP as above.

Human tissue samples. Postmortem optic nerve samples from 13 long-standing MS patients and 12 control subjects (who died from non-neurological diseases) were obtained at autopsy under the management of the Netherlands Brain Bank. All patients and controls had previously given written approval for the use of their tissue, according to the guidelines of the Netherlands Brain Bank. Clinical characteristics of the control and patient groups together with macroscopic tissue analysis to characterize MS samples were as reported previously (Vallejo-Illarramendi et al., 2006). For comparisons, MS samples were matched with control samples for age, sex, and postmortem delay. Double immunofluorescence and Western blot were performed as for rat tissues except for the antibodies to $P2X_7$, which were against the extracellular part of the receptor (2 μg/ml; Alomone Labs). CD68 antibodies to macrophage/microglia (DakoCytomation) were used at 10 μg/ml. Hoechst 33258 (5 μg/ml; Sigma) was used for chromatin staining.

Real-time quantitative PCR. Primers specific for the $P2X_7$ receptor were designed with PrimerExpress software (Applied Biosystems, Madrid, Spain). Real-time quantitative PCR reactions were performed in an ABI PRISM 7000 Sequence Detection System instrument (Applied Biosystems) as described previously (Vallejo-Illarramendi et al., 2006) .

Statistical analysis. Data are presented as mean ± SEM. The significance between two datasets was tested with the unpaired *t* test, except for *in vitro* toxicity assays, which were tested with a paired *t* test. For symptom scores in EAE experiments, significance between each two groups was examined using the Mann–Whitney *U* test. For multiple comparisons in the neurophysiological assessment assays, we use ANOVA (Tukey's *post hoc*). In all instances, a value of $p < 0.05$ was considered significant.

Results

Oligodendrocytes express functional $P2X_7$ receptors

We initially examined whether oligodendrocytes in culture respond to ATP. In normal extracellular solution, ATP (1 mM) induced a nondesensitizing inward current (Fig. 1*A*) in most oligodendrocytes (77.3 ± 7.9%; $n = 47$) with an amplitude ranging from −8 to −60 pA (−20.9 ± 4.2 pA; $n = 36$). The ATP analog BzATP (100 μM), a $P2X_1$, $P2X_2$, and $P2X_7$ receptor agonist (Khakh et al., 2001), induced similar responses (−17.8 ± 5.7 pA; $n = 14$) (Fig. 1*A*). In contrast, α,β-methylene-ATP (α,β-meATP) (100 μM), a selective agonist of $P2X_1$, $P2X_3$, and heteromeric $P2X_{2/3}$ receptors (Khakh et al., 2001), did not elicit any response ($n = 8$) (Fig. 1*A*). ATP-induced currents were mediated by receptors with low affinity for ATP (EC_{50} of 8.8 mM; $n = 21$) (Fig. 1*A*). BzATP was an order of magnitude more potent than ATP (EC_{50} of 0.5 mM; $n = 7$) (Fig. 1*A*), a characteristic specific of $P2X_7$ receptors (el-Moatassim and Dubyak, 1992). In the absence of Mg^{2+} and Ca^{2+}, which results in an increase in the concentration of ATP^{4-}, the active form of ATP at most P2X receptors, ATP- and BzATP-induced currents were strongly potentiated and had an EC_{50} of 873.2 μM ($n = 10$) and 99 μM ($n = 12$), respectively (Fig. 1*A*). Moreover, pyridoxal phosphate 6-azophenyl-2′,4′-disulphonic acid (PPADS) (100 μM), a nonselective antagonist of P2X receptors, completely abolished inward currents mediated by ATP ($n = 7$) (Fig. 1*A*). These findings indicate that oligodendrocytes express functional P2X receptors.

We then tested the effects of different P2X antagonists on ATP-induced inward currents. Periodate oATP (1 mM), a preferential antagonist of $P2X_7$ receptors (Murgia et al., 1993), almost completely blocked ATP (70.6 ± 6.9% inhibition; $n = 18$) (Fig.

1*B*) and BzATP-induced currents in Ca^{2+} and Mg^{2+}-free conditions (81.8 ± 3.8% inhibition; $n = 13$) (Fig. 1*B*). In addition, BBG, a potent $P2X_7$ antagonist, nearly abolished ATP (10 mM; $n = 30$) and BzATP (1 mM; $n = 8$) currents at concentrations (IC_{50} values of 30 and 17 nM, respectively) (Fig. 1*C*) that do not affect other P2X subtypes (Jiang et al., 2000). This pharmacological profile indicates that $P2X_7$ receptors are major mediators of ATP responses in oligodendrocytes, an idea that is supported by the fact that $P2X_7^{-/-}$ oligodendrocytes *in vitro* have very small responses to ATP and BzATP (supplemental Fig. 1*A*, available at www.jneurosci.org as supplemental material).

To characterize further the functional properties of $P2X_7$ receptors, we next monitored the concentration of intracellular calcium $[Ca^{2+}]_i$ after application of ATP and BzATP to cultured oligodendrocytes. We found that application of ATP (1 mM) caused a rapid increase in cytosolic Ca^{2+} (358 ± 28 nM; $n = 33$), which is greatly reduced (57 ± 2 nM; $n = 10$) in the absence of Ca^{2+} in the incubation buffer and completely blocked by PPADS (50 μM; $n = 5$) (Fig. 1*D*,*E*). Similar results were obtained with BzATP (1 mM) (Fig. 1*D*,*E*). These results indicate that $[Ca^{2+}]_i$ increase is mainly attributable to Ca^{2+} influx through the plasma membrane and marginally to Ca^{2+} release from intracellular stores. In addition, the ATP-induced $[Ca^{2+}]_i$ increase was reduced to 70 ± 3%, ($n = 25$) and 31 ± 15% ($n = 24$), respectively (Fig. 1*D*,*E*), by BBG at concentrations that selectively block $P2X_7$ receptors (10 and 100 nM) (Jiang et al., 2000). Consistently, the ATP and BzATP (both at 1 mM) responses were substantially reduced by oATP (49 ± 15 and 39 ± 11%, respectively; $n = 10$ each) (Fig. 1*D*,*E*).

To localize the expression of P2X receptor subunits in oligodendrocytes, we performed Western blot and double-immunofluorescence labeling of cultured myelin basic protein-positive oligodendrocytes (MBP^+ cells), as well as rat optic nerve and spinal cord sections with subunit-specific antibodies to P2X receptors and with the oligodendrocyte marker APC (Bhat et al., 1996). Immunoblotting revealed that the 75 kDa band corresponding to the $P2X_7$ receptor is present in the rat optic nerve as well as in cultured oligodendrocytes from this structure (Fig. 2*A*) but absent in $P2X_7^{-/-}$ mice optic nerve and oligodendrocytes (supplemental Fig. 1*B*, available at www.jneurosci.org as supplemental material). In turn, double-immunofluorescence staining showed that $P2X_7$ is heavily expressed in cultured oligodendrocytes and in the optic nerve and spinal cord (Fig. 2*B*) (supplemental Fig. 2, available at www.jneurosci.org as supplemental material). In contrast, no immunolabeling with antibodies to the $P2X_7$ receptor was observed in optic nerve from $P2X_7^{-/-}$ mice (supplemental Fig. 1*C*, available at www.jneurosci.org as supplemental material). Moreover, immunogold electron microscopy revealed that this receptor is also located in myelin sheaths (5.14 ± 0.84 gold particles/μm^2) (Fig. 2*C*). In addition to $P2X_7$, $P2X_2$ and $P2X_4$, but not $P2X_1$, are also present in oligodendrocytes both *in vitro* and *in situ* (supplemental Table 1, available at www.jneurosci.org as supplemental material).

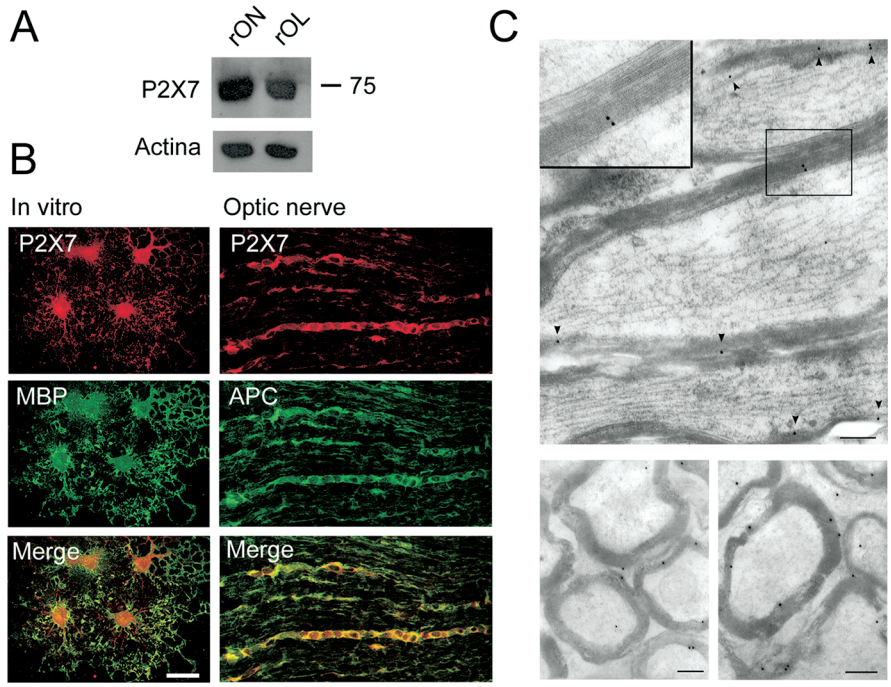

Figure 2. $P2X_7$ receptors are expressed in oligodendrocytes and myelin. ***A***, Western blot illustrating the presence of $P2X_7$ receptor in rat optic nerve (rON) and rat oligodendrocytes in culture (rOL). ***B***, $P2X_7$ receptors revealed by double-immunofluorescence labeling in rat MBP^+ oligodendrocytes in culture (left column) and in optic nerve APC^+ oligodendrocytes (right column). Scale bar, 20 μm. ***C***, Electron microscopic images of longitudinal (top) and transversal (bottom) sections showing immunogold staining of $P2X_7$ receptors in myelin sheaths (inset and arrowheads). Scale bars, 300 nm.

Together, these results indicate that P2X receptors in oligodendrocytes have electrophysiological, pharmacological, and molecular properties compatible with a predominant expression of $P2X_7$ and demonstrate that this receptor is a major mediator of $[Ca^{2+}]_i$ elevation triggered by ATP.

$P2X_7$ receptor activation induces oligodendrocyte death

AMPA and kainate receptor activation in oligodendrocytes causes an increase in basal $[Ca^{2+}]_i$ levels, which results in oligodendrocyte death (Alberdi et al., 2002). Because $P2X_7$ receptors in oligodendrocytes are also highly permeable to Ca^{2+} and do not desensitize, we tested whether activation of these receptors can kill these cells. We observed that addition to the cultures of ATP (1 mM) or BzATP (10 μM) for 15 min was toxic to $O4/GalC^+$ oligodendrocytes (Fig. 3*A*). In turn, MBP^+ oligodendrocytes after 5 d *in vitro* were similarly vulnerable to both agonists (data not shown). ATP and BzATP toxicity was prevented by removal of Ca^{2+} from the culture media and by the nonselective P2X receptor antagonist PPADS (50 μM), as well as by oATP and BBG at concentrations that selectively block $P2X_7$ receptors (300 μM and 50 nM, respectively) (Fig. 3*A*). ATP-γ-S, a more stable analog of ATP, was also toxic to oligodendrocytes (supplemental Fig. 3, available at www.jneurosci.org as supplemental material).

To determine whether ATP can kill oligodendrocytes *in situ*, we perfused whole optic nerves freshly isolated from adult rats with oxygen-saturated aCSF alone or with ATP (1 mM) for 3 h. Basal chromatin condensation in the nerves under control experimental conditions was very low. In contrast, ATP increased approximately threefold the number of cells showing condensed nuclei ($n = 6$). These cells were typically oriented in the longitu-

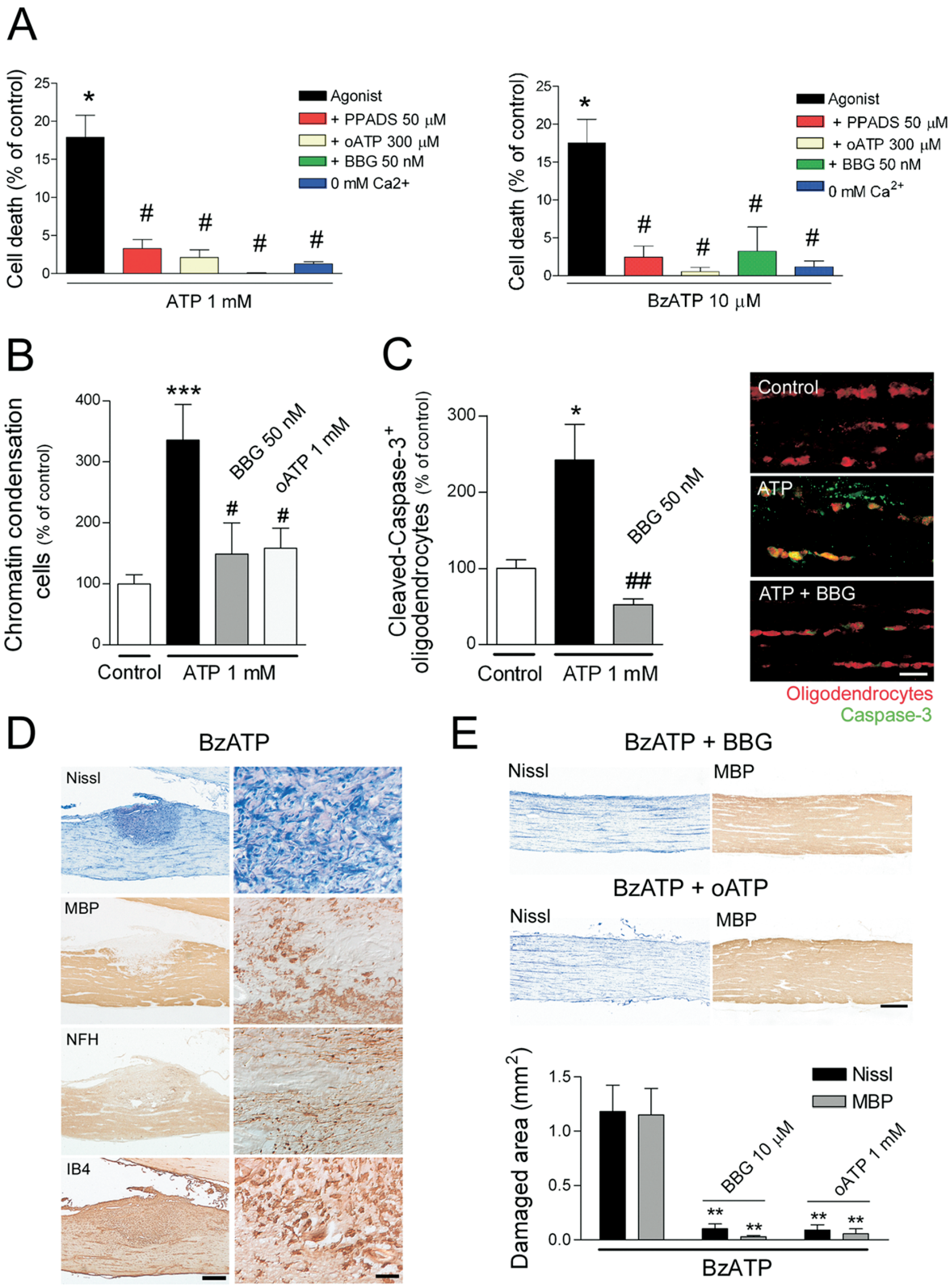

Figure 3. P2X receptor activation triggers oligodendrocyte death in dissociated cultures and in isolated optic nerve *in vitro*, as well as MS-like lesions *in vivo*. ***A***, Toxicity of ATP (left) and BzATP (right) in optic nerve oligodendrocytes in culture, as measured 24 h later with the calcein viability assay. Oligodendrocyte death is observed after exposure to ATP and BzATP at 1 mM and 10 μM, respectively (*$p < 0.05$ for comparison between agonist and control). This is prevented by coapplication of the broad-spectrum P2X antagonist PPADS, by $P2X_7$ receptor antagonists oATP and BBG, and by Ca^{2+} removal from the culture medium ($^{\#}p < 0.05$ for each comparison between agonist and the various conditions). ***B***, ***C***, Perfusion of rat optic nerves with aCSF-containing ATP results in chromatin condensation and caspase-3 activation in oligodendrocytes labeled with APC, an effect that is prevented by coapplication with $P2X_7$ antagonists. Scale bar, 10 μm. *$p < 0.05$, ***$p < 0.001$ for comparison between control and treatment with agonist; $^{\#}p < 0.05$, $^{\#\#}p < 0.01$ for comparison between agonist and agonist plus antagonist treatment. ***D***, BzATP slowly infused onto the rabbit optic nerve induces defined lesions with microgliosis [isolectin B4 (IB4)] as well as demyelination and axonal damage, as shown by staining with antibodies to MBP and dephosphorylated NFH, respectively. Left and right panels correspond to low and high magnification of damaged nerves, respectively (scale bars, 500 and 50 μm). ***E***, BzATP-induced lesions are prevented by coapplication of $P2X_7$ antagonists BBG or oATP. Scale bar, 500 μm. The histogram shows the extent of damaged and demyelinated area attributable to BzATP application and its reduction with BBG and oATP. **$p < 0.01$.

dinal axis of the nerve, forming part of cell rows that were identified as being made up of interfascicular oligodendrocytes. Cell death was prevented in the presence of $P2X_7$ antagonists oATP (1 mM; $n = 3$) and by BBG (50 nM; $n = 3$) (Fig. 3*B*). Consistent with these findings, we observed that ATP-treated optic nerves showed numerous cleaved caspase-3$^+$ oligodendrocytes, identified by APC immunostaining, which were absent in nerves exposed to ATP in the presence of BBG (50 nM; $n = 3$) (Fig. 3*C*).

We next infused optic nerves *in vivo* with BzATP ($n = 5$) or vehicle (saline, $n = 10$) using osmotic pumps that delivered trace amounts of agonists for 3 d. Histological examination of the nerves 7 d after initiating the application showed no alterations in the saline group. In contrast, nerves treated with agonists presented tissue damage, intense microgliosis, loss of MBP near the site at which the cannula tip was located, and aggregates of dephosphorylated NFH, which extended well into the optic chiasm and which were indicative of axonal damage ($n = 6$) (Fig. 3*D*,*E*). Similar tissue alterations were observed using ATP-γ-S ($n = 4$; data not shown). All these features are reminiscent of MS lesions. This damage was prevented by coapplication of agonists with BBG ($n = 4$) and oATP ($n = 6$) (Fig. 3*E*).

Altogether, our toxicity assays showed that oligodendrocytes are similarly vulnerable to P2X activation by ATP and BzATP, an effect that was prevented by $P2X_7$ antagonists both *in vitro* and *in vivo*. In addition, the lesions *in vivo* are strikingly reminiscent of those found in MS.

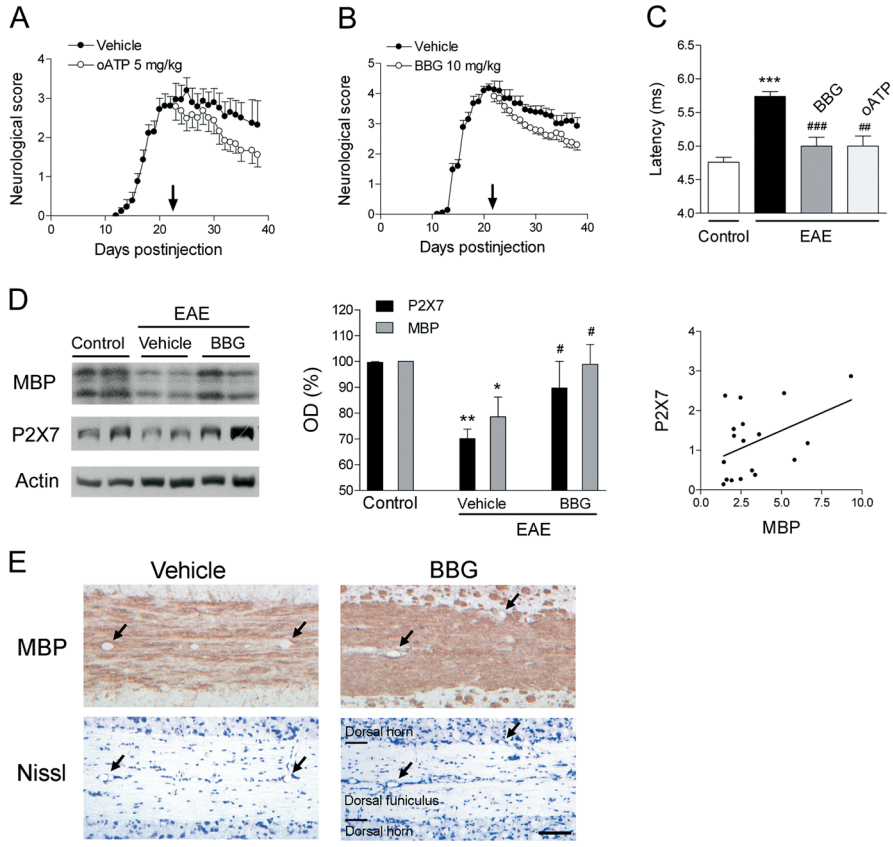

Figure 4. $P2X_7$ antagonists ameliorate chronic EAE-associated neurological symptoms and restore normal axon conduction velocity. ***A***, ***B***, Established chronic EAE induced in C57BL/6 mice by immunization with MOG improves after treatment with oATP ($p < 0.001$) and BBG ($p < 0.01$) starting at 21 d after injection (arrows). ***C***, The increase in axon conduction latency in the corticospinal tract of mice with chronic EAE ($^{***}p < 0.001$ vs control, non-immunized animals) is greatly attenuated after treatment with oATP and BBG ($^{\#\#}p < 0.01$ and $^{\#\#\#}p < 0.001$, respectively, compared with MOG immunized mice). ***D***, Immunoblotting with tissue samples from lumbar spinal cord of mice with chronic EAE (left) and corresponding histogram (middle; OD, optic density) show a decrease in the levels of MBP and $P2X_7$ receptor that is inhibited by BBG. Sample loading was normalized to actin levels. Symbols in histogram denote a statistically significant reduction of protein levels in vehicle-treated mice versus control, non-immunized mice ($^*p < 0.05$ and $^{**}p < 0.01$) and an increase in BBG-treated mice versus the vehicle group ($^{\#}p < 0.05$). $P2X_7$ levels (right) correlate with those of MBP ($r = 0.44$ and $p < 0.05$, Pearson's correlation). ***E***, Nissl and MBP immunostaining of consecutive longitudinal sections from the lumbar spinal cord of mice with chronic EAE. Arrows point to same blood vessels. Demyelination is evident in mice treated with vehicle but not in mice treated with $P2X_7$ antagonist BBG. Nissl staining reveals that demyelination in the former mice may also occur in the absence of signs of inflammation. Scale bar, 100 μm. Data shown in ***C–E*** were obtained at 40 dpi.

$P2X_7$ receptor antagonism attenuates EAE

We then evaluated the efficacy of $P2X_7$ antagonists in ameliorating the symptoms associated with chronic EAE induced in C57BL/6 mice, a model that is relevant to the chronic and progressive phase of MS, after the disease onset and when the neurological score was maximal. Mice immunized with MOG experienced motor deficits that commenced at ~12 dpi. Treatment with oATP or BBG (5 and 10 mg/kg daily; $n = 28$ and 21, respectively) starting at 21 dpi ameliorated the motor deficits observed in vehicle-treated animals ($n = 30$) (Fig. 4*A*,*B*). Moreover, the latency of the corticospinal tract at the end of the experiment (40 dpi) was 5.74 ± 0.08 ms in immunized animals treated with vehicle ($n = 30$), whereas in those treated with oATP ($n = 24$) or BBG ($n = 8$), latency values were 5.01 ± 0.15 or 5 ± 0.13 ms, respectively, which was close to that measured in control, non-immunized animals 4.76 ± 0.08 ms ($n = 15$) (Fig. 4*C*). In addition, $P2X_7$ and MBP levels at 40 dpi decreased (Fig. 4*D*) in animals with chronic EAE treated with vehicle ($n = 8$), although these levels were similar to controls in EAE animals treated with BBG ($n = 8$); indeed, both parameters were correlated. Notably, MBP immunohistochemistry in vehicle-treated animals at 40 dpi showed demyelinated areas typically associated with inflammation but also in the absence of it (Fig. 4*E*). In contrast, demyelination was greatly reduced in EAE mice treated with $P2X_7$ antagonists (Fig. 4*E*). Altogether, these results demonstrate that $P2X_7$ blockade ameliorates chronic EAE by reducing demyelination and thus improving axonal conduction.

Increased $P2X_7$ expression in multiple sclerosis

We next examined whether human oligodendrocytes express $P2X_7$ receptors by double-immunofluorescence staining in optic nerve samples obtained at autopsy. We found that $P2X_7$ receptors were located in the cell body and proximal processes of oligodendrocytes both in samples of optic nerves from controls and from MS patients that had a normal histological appearance of the nerve ($n = 5$) (Fig. 5*A*). In addition, we observed immunolabeling in cells of the microglia/macrophage lineage (Fig. 5*A*). Subsequently, we measured the levels of $P2X_7$ mRNA in a cohort of

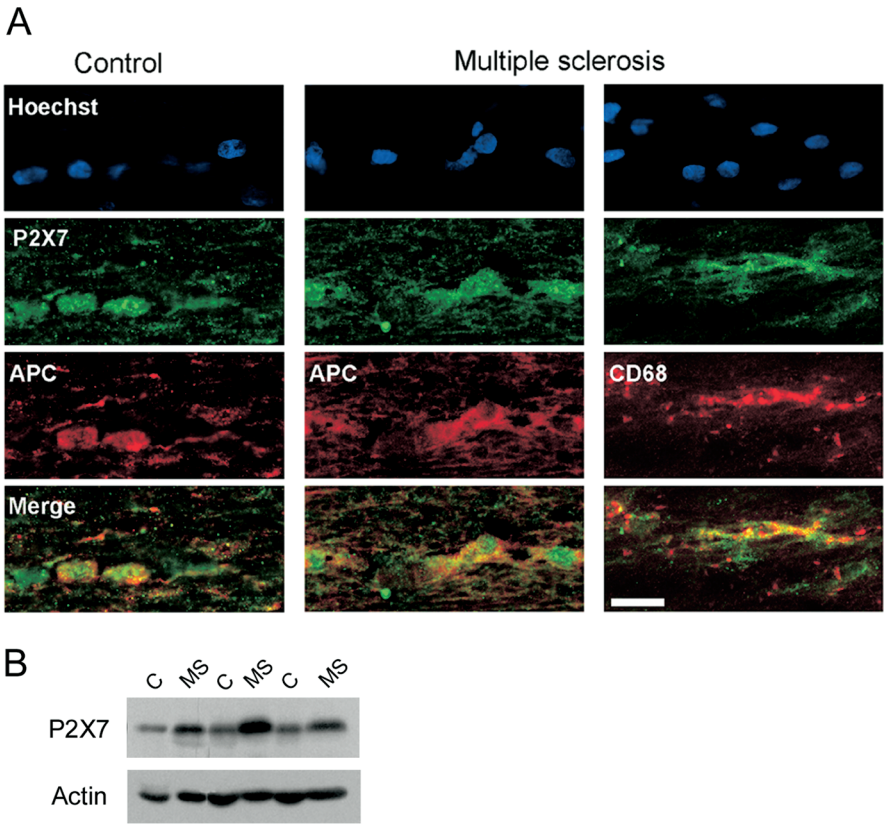

Figure 5. $P2X_7$ receptor levels are increased in MS. ***A***, Hoechst (top) and immunofluorescence staining of oligodendrocytes (APC^+ cells) with antibodies to $P2X_7$ receptors in the human optic nerve from controls and normally appearing MS samples. Merge images show that $P2X_7$ receptors are located in oligodendrocytes in both control and MS samples. In turn, cells of the microglial lineage ($CD68^+$) also show $P2X_7$ immunolabeling. Scale bar, 20 μm. ***B***, Western blot of optic nerve homogenates from sex- and age-matched controls (C) and MS cases. Sample loading was normalized to the intensity of bands corresponding to actin.

previously characterized MS samples (Vallejo-Illarramendi et al., 2006). Interestingly, real-time quantitative PCR experiments showed an increase of 70.1 ± 48.2% in the levels of $P2X_7$ mRNA in normally appearing optic nerve MS samples ($n = 6$; $p < 0.05$ with respect to age- and sex-matched controls). These results were confirmed by Western blot assays (Fig. 5*B*) that showed an increase of 104.2 ± 53.1% in the levels of $P2X_7$ protein ($n = 7$; $p < 0.05$ with respect to age- and sex-matched controls). Together, these findings indicate that $P2X_7$ signaling is enhanced in normal-appearing axonal tracts of the CNS in MS, and thus, this feature may make oligodendrocytes more vulnerable to primary or secondary alterations in early lesion formation in this disease.

Discussion

The data reported here indicate that oligodendrocytes are vulnerable to sustained activation of $P2X_7$ receptors and that $P2X_7$ antagonists attenuate tissue damage and the neurological consequences associated with EAE. Furthermore, the elevated expression of $P2X_7$ receptors in oligodendrocytes in normal-appearing axon tracts in MS suggests that this feature may be a risk factor associated with early lesion formation in this disease.

In neurons, $P2X_7$ receptors constitute a large source of transmitter-activated Ca^{2+} influx (North, 2002; Egan and Khakh, 2004). In turn, $P2X_7$ are also expressed in glial cells including astrocytes, microglia, and Schwann cells (North, 2002). In addition, recent studies provided preliminary evidence showing that oligodendrocytes and their progenitors express $P2X_7$ receptors *in vitro* (James and Butt, 2002; Agresti et al., 2005). In agreement with those results, we found that differentiated oligodendrocytes have a robust expression of P2X receptors whose electrophysiological, pharmacological, and molecular properties *in vitro* and *in vivo* correspond to that of the $P2X_7$ subtype. Notably, Ca^{2+} influx subsequent to $P2X_7$ activation is very high, a feature that renders oligodendrocytes vulnerable to intense signaling through this receptor. Indeed, sustained activation of $P2X_7$ receptors by ATP and BzATP is lethal to oligodendroglia and causes severe tissue damage. Likewise, excitotoxicity-based neuronal degeneration triggered by $P2X_7$ receptors has been described recently after ischemia (Le Feuvre et al., 2003) and subsequent to spinal cord injury (Wang et al., 2004). However, we cannot exclude the possibility that $P2X_2$ and $P2X_4$ receptors, which are also present in oligodendrocytes, contribute to some of the observed ATP toxicity in these cells.

These observations are in line with previous findings illustrating that enhanced activation of AMPA and kainate as well as NMDA receptors in oligodendrocytes induces calcium overload and ultimately cell death (Matute et al., 2001; Alberdi et al., 2002; Goldberg and Ransom, 2003; Karadottir et al., 2005; Salter and Fern, 2005; Micu et al., 2006). Glutamate excitotoxicity is indeed relevant to white matter damage in acute diseases such as stroke (Goldberg and Ransom, 2003) and also in animal models of MS including EAE (Pitt et al., 2000; Smith et al., 2000). In these pathological conditions, antagonists of ionotropic glutamate receptors protect against tissue loss and attenuate the functional deficits associated with white matter destruction (Pitt et al., 2000; Smith et al., 2000; Goldberg and Ransom, 2003). Likewise, our findings in EAE experiments strongly suggest that blockade of $P2X_7$ receptors protects against myelin loss and attenuates the functional decline associated with the disease. In turn, modulation of the immune response by $P2X_7$ antagonists could also contribute to amelioration of EAE symptoms, but this possibility is not supported by the fact that the severity of EAE is exacerbated in $P2X_7^{-/-}$ mice (Chen and Brosnan, 2006).

ATP, the endogenous agonist of $P2X_7$ receptors, is an important signaling molecule in nonsynaptic regions (Hansson and Rönnbäck, 2003). Although $P2X_7$ receptors have relatively low affinity for ATP, the extracellular concentration of this nucleotide increases significantly in response to injury (Anderson and Nedergaard, 2006). Thus, spinal cord trauma causes the release of ATP around the damaged area, as measured by bioluminescence, and results in cell death of nearby neurons and oligodendrocytes that is strongly attenuated by $P2X_7$ antagonists (Wang et al., 2004). In addition, other studies have shown that trauma liberates large amounts of ATP (Nieber et al., 1999; Ray et al., 2002) (for review, see Anderson and Nedergaard, 2006).

There are several tissue compartments that can contribute to elevate extracellular levels of ATP and thus induce direct or indi-

rect $P2X_7$-mediated damage in EAE. With an intracellular ATP concentration in the millimolar range, injured cells in EAE have the potential to release large amounts of ATP and directly trigger oligodendrocyte and myelin destruction, as observed when ATP and BzATP are administered directly onto the optic nerve (Fig. 3*B–D*). ATP can also be released from astrocytes by activation of $P2X_7$ receptors (Suadicani et al., 2006). Finally, infiltrating cells of the monocyte/macrophage lineage and activated microglia can release ATP (Sperlagh et al., 1998; Seo et al., 2004) and thus contribute to $P2X_7$ activation and cell death in oligodendrocytes.

In addition to its direct deleterious effects on oligodendrocyte survival, ATP can also activate signaling cascades in astrocytes and microglia, which leads to oligodendrocyte death. Thus, ATP is a potent activator of astrocytic glutamate release (Jeremic et al., 2001; Nedergaard et al., 2002), in particular by activation of $P2X_7$ receptors (Duan et al., 2003), which in turn can cause oligodendrocyte excitotoxicity and thus create a deleterious loop that could be halted by $P2X_7$ receptor antagonists. Conversely, ATP can stimulate microglial cells and invading macrophages recruited during immune attack of the CNS, to release toxic agents including interleukin-1β (IL-1β), tumor necrosis factor-α, and superoxide and nitric oxide (Solle et al., 2001; Parvathenani et al., 2003; Block and Hong, 2005), all of which may contribute to oligodendrocyte demise. Indeed, $P2X_7$ receptor blockade attenuates lipopolysaccharide-induced microglial activation and confers neuroprotection in inflamed brain (Choi et al., 2007).

Signaling through the $P2X_7$ receptor is upregulated in activated microglia surrounding β-amyloid plaques in a mouse model of Alzheimer's disease (Parvathenani et al., 2003). Interestingly, the proinflammatory cytokine IL-1β enhances $P2X_7$ receptor expression and function in astrocytes (Narcisse et al., 2005). Thus, increased levels of IL-1β in MS and its animal model EAE (Hauser et al., 1990) can intensify signaling through the $P2X_7$ receptor and lead to the release of ATP and glutamate, which causes oligodendrocyte excitotoxicity. This may be relevant to the progression of tissue damage in normal-appearing white matter in MS because, in the chronic state of the disease, diffuse inflammation accumulates throughout the whole brain and is associated with slowly progressive axonal injury (Kutzelnigg et al., 2005). However, it should be noticed that, in contrast to the proinflammatory role of $P2X_7$ receptors within the CNS, these receptors also mediate apparently opposite effects in the immune system because EAE symptoms are exacerbated in $P2X_7^{-/-}$ mice (Chen and Brosnan, 2006).

In summary, we have shown here that enhanced ATP signaling *in vitro* and *in vivo* leads to oligodendrocyte death via $P2X_7$ receptor-mediated Ca^{2+} toxicity and that $P2X_7$ receptors mediate tissue damage underlying the neurological deficits associated with well established models of MS. In turn, the increased expression of $P2X_7$ receptors in axon tracts before lesions are formed in MS suggests that this feature constitutes a risk factor associated with newly forming lesions in this disease. Blockade of ATP $P2X_7$ receptors has potent neuroprotective properties, suggesting that this mechanism could be exploited to halt the progression of tissue damage in MS.

References

Agresti C, Meomartini ME, Amadio S, Ambrosini E, Serafini B, Franchini L, Volonte C, Aloisi F, Visentin S (2005) Metabotropic P2 receptor activation regulates oligodendrocyte progenitor migration and development. Glia 50:132–144.

Alberdi E, Sánchez-Gómez MV, Marino A, Matute C (2002) Ca^{2+} influx through AMPA or kainate receptors alone is sufficient to initiate excitotoxicity in cultured oligodendrocytes. Neurobiol Dis 9:234–243.

Anderson CM, Nedergaard M (2006) Emerging challenges of assigning P2X7 receptor function and immunoreactivity in neurons. Trends Neurosci 29:257–262.

Barres BA, Hart IK, Coles HS, Burne JF, Voyvodic JT, Richardson WD, Raff MC (1992) Cell death and control of cell survival in the oligodendrocyte lineage. Cell 70:31–46.

Bhat RV, Axt KJ, Fosnaugh JS, Smith KJ, Johnson KA, Hill DE, Kinzler KW, Baraban JM (1996) Expression of the APC tumor suppressor protein in oligodendroglia. Glia 17:169–174.

Block ML, Hong JS (2005) Microglia and inflammation-mediated neurodegeneration: multiple triggers with a common mechanism. Prog Neurobiol 76:77–98.

Burnstock G (1972) Purinergic nerves. Pharmacol Rev 24:509–581.

Chen L, Brosnan CF (2006) Exacerbation of experimental autoimmune encephalomyelitis in P2X7R−/− mice: evidence for loss of apoptotic activity in lymphocytes. J Immunol 170:3115–3126.

Choi HB, Ryu JK, Kim SU, McLarnon JG (2007) Modulation of the purinergic $P2X_7$ receptor attenuates lipopolysaccharide-mediated microglial activation and neuronal damage in inflamed brain. J Neurosci 27:4957–4968.

Di Virgilio F, Sanz JM, Chiozz P, Falzoni S (1999) The P2Z/P2X7 receptor of microglial cells: a novel immunomodulatory receptor. Prog Brain Res 120:355–368.

Duan S, Anderson CM, Keung EC, Chen Y, Chen Y, Swanson RA (2003) $P2X_7$ receptor-mediated release of excitatory amino acids from astrocytes. J Neurosci 23:1320–1328.

Egan TM, Khakh BS (2004) Contribution of calcium ions to P2X channel responses. J Neurosci 24:3413–3420.

el-Moatassim C, Dubyak GR (1992) A novel pathway for the activation of phospholipase D by P2z purinergic receptors in BAC1.2F5 macrophages. J Biol Chem 267:23664–23673.

Goldberg MP, Ransom BR (2003) New light on white matter. Stroke 34:330–332.

Groom AJ, Smith T, Turski L (2003) Multiple sclerosis and glutamate. Ann NY Acad Sci 993:229–275.

Grynkiewikcz G, Poenie M, Tsien RY (1985) A new generation of Ca^{2+} indicators with greatly improved fluorescence properties. J Biol Chem 260:3440–3450.

Hansson E, Rönnbäck L (2003) Glial neuronal signaling in the central nervous system. FASEB J 17:341–348.

Hauser SL, Doolittle TH, Lincoln R, Brown RH, Dinarello CA (1990) Cytokine accumulations in CSF of multiple sclerosis patients: frequent detection of interleukin-1 and tumor necrosis factor but not interleukin-6. Neurology 40:1735–1739.

James G, Butt AM (2002) P2Y and P2X purinoceptor mediated Ca^{2+} signalling in glial cell pathology in the central nervous system. Eur J Pharmacol 447:247–260.

Jeremic A, Jeftinija K, Stevanovic J, Glavaski A, Jeftinija S (2001) ATP stimulates calcium-dependent glutamate release from cultured astrocytes. J Neurochem 77:664–675.

Jiang L-H, Mackenzie AB, North RA, Surprenant A (2000) Brilliant blue G selectively blocks ATP-gated rat P2X(7) receptors. Mol Pharmacol 58:82–88.

Karadottir R, Cavelier P, Bergersen LH, Attwell D (2005) NMDA receptors are expressed in oligodendrocytes and activated in ischaemia. Nature 438:1162–1166.

Khakh BS (2001) Molecular physiology of P2X receptors and ATP signaling at synapses. Nat Rev Neurosci 2:165–174.

Khakh BS, Burnstock G, Kennedy C, King BF, North RA, Seguela P, Voigt M, Humphrey PP (2001) International Union of Pharmacology. XXIV. Current status of the nomenclature and properties of P2X receptors and their subunits. Pharmacol Rev 53:107–118.

Kutzelnigg A, Lucchinetti CF, Stadelmann C, Bruck W, Rauschka H, Bergmann M, Schmidbauer M, Parisi JE, Lassmann H (2005) Cortical demyelination and diffuse white matter injury in multiple sclerosis. Brain 128:2705–2712.

Lassmann H (2005) Multiple sclerosis pathology: evolution of pathogenetic concepts. Brain Pathol 15:217–222.

Le Feuvre RA, Brough D, Touzani O, Rothwell NJ (2003) Role of P2X7 receptors in ischemic and excitotoxic brain injury in vivo. J Cereb Blood Flow Metab 23:381–384.

Matute C (1998) Characteristics of acute and chronic kainate excitotoxic damage to the optic nerve. Proc Natl Acad Sci USA 18:10229–10234.

Matute C, Sánchez-Gómez MV, Martínez-Millán L, Miledi R (1997) Glutamate receptor mediated toxicity in optic nerve oligodendrocytes. Proc Natl Acad Sci USA 94:8830–8835.

Matute C, Alberdi E, Domercq M, Pérez-Cerdá F, Pérez-Samartín A, Sánchez-Gómez MV (2001) The link between excitotoxic oligodendroglial death and demyelinating diseases. Trends Neurosci 24:224–230.

Micu I, Jiang Q, Coderre E, Ridsdale A, Zhang L, Woulfe J, Yin X, Trapp BD, McRory JE, Rehak R, Zamponi GW, Wang W, Stys PK (2006) NMDA receptors mediate calcium accumulation in myelin during chemical ischaemia. Nature 439:988–992.

Murgia M, Hanau S, Pizzo P, Rippa M, Di Virgilio F (1993) Oxidized ATP. An irreversible inhibitor of the macrophage purinergic P2Z receptor. J Biol Chem 268:8199–8203.

Narcisse L, Scemes E, Zhao Y, Lee SC, Brosnan CF (2005) The cytokine IL-1beta transiently enhances P2X7 receptor expression and function in human astrocytes. Glia 49:245–258.

Nedergaard M, Takano T, Hansen AJ (2002) Beyond the role of glutamate as a neurotransmitter. Nat Rev Neurosci 3:748–755.

Nieber K, Eschke D, Brand A (1999) Brain hypoxia: effects of ATP and adenosine. Prog Brain Res 120:287–297.

North RA (2002) Molecular physiology of P2X receptors. Physiol Rev 82:1013–1067.

Parvathenani LK, Tertyshnikova S, Greco CR, Roberts SB, Robertson B, Posmantur R (2003) P2X7 mediates superoxide production in primary microglia and is up-regulated in a transgenic mouse model of Alzheimer's disease. J Biol Chem 278:13309–13317.

Pitt D, Werner P, Raine CS (2000) Glutamate excitotoxicity in a model of multiple sclerosis. Nat Med 6:67–70.

Prineas JW, McDonald WI, Franklin RJM (2002) Demyelinating diseases. In: Greenfield's neuropathology, Vol 2 (Graham DI, Lantos PL, eds), pp 471–550. London: Arnold.

Ralevic V, Burnstock G (1998) Receptors for purines and pyrimidines. Pharmacol Rev 50:413–492.

Ray SK, Dixon CE, Banik NL (2002) Molecular mechanisms in the pathogenesis of traumatic brain injury. Histol Histopathol 17:1137–1152.

Rubio ME, Soto F (2001) Distinct localization of P2X receptors at excitatory postsynaptic specializations. J Neurosci 21:641–653.

Salter MG, Fern R (2005) NMDA receptors are expressed in developing oligodendrocyte processes and mediate injury. Nature 438:1167–1171.

Sánchez-Gómez MV, Matute C (1999) AMPA and kainate receptors each mediate excitotoxicity in oligodendroglial cultures. Neurobiol Dis 6:475–485.

Sánchez-Gómez MV, Alberdi E, Ibarretxe G, Torre I, Matute C (2003) Caspase-dependent and caspase-independent oligodendrocyte death mediated by AMPA and kainate receptors. J Neurosci 23:9519–9528.

Seo DR, Kim KY, Lee YB (2004) Interleukin-10 expression in lipopolysaccharide-activated microglia is mediated by extracellular ATP in an autocrine fashion. NeuroReport 15:1157–1161.

Smith T, Groom A, Zhu B, Turski L (2000) Autoimmune encephalomyelitis ameliorated by AMPA antagonists. Nat Med 6:62–66.

Solle M, Labasi J, Perregaux DG, Stam E, Petrushova N, Koller BH, Griffiths RJ, Gabel CA (2001) Altered cytokine production in mice lacking P2X(7) receptors. J Biol Chem 276:125–132.

Somogyi P, Soltész I (1986) Immunogold demonstration of GABA in synaptic terminals of intracellularly recorded, horseradish peroxidase-filled basket cells and clutch cells in the cat's visual cortex. Neuroscience 19:1051–1065.

Sperlagh B, Hasko G, Nemeth Z, Vizi ES (1998) ATP released by LPS increases nitric oxide production in raw 264.7 macrophage cell line via P2Z/P2X7 receptors. Neurochem Int 33:209–215.

Steinman L (2001) Multiple sclerosis: a two-stage disease. Nat Immunol 2:762–764.

Suadicani SO, Brosnan CF, Scemes E (2006) P2X7 receptors mediate ATP release and amplification of astrocytic intercellular Ca^{2+} signaling. J Neurosci 26:1378–1385.

Torres G, Egan T, Voigt M (1999) Hetero-oligomeric assembly of P2X receptor subunits: specificities exist with regard to possible partners. J Biol Chem 274:6653–6659.

Vallejo-Illarramendi A, Domercq M, Pérez-Cerdá F, Ravid R, Matute C (2006) Increased expression and function of glutamate transporters in multiple sclerosis. Neurobiol Dis 21:154–164.

Wang X, Arcuino G, Takano T, Lin J, Peng WG, Wan P, Li P, Xu Q, Liu QS, Goldman SA, Nedergaard M (2004) P2X7 receptor inhibition improves recovery after spinal cord injury. Nat Med 10:821–827.

Zamvil SS, Steinman L (2003) Diverse targets for intervention during inflammatory and neurodegenerative phases of multiple sclerosis. Neuron 38:685–688.